BMC Neuroscience

RESEARCH

Open Access

Body weight-supported treadmill training reduces glial scar overgrowth in SCI rats by decreasing the reactivity of astrocytes during the subacute phase

Jili Cai[1†], Yu Wang[1†], Chenyuan Zhai[2†], Kunmao Jiang[3], Zun Wang[4], Lu Fang[1], Xiangzhe Li[1,5], Chenchen Zhu[1], Wentao Liu[3], Tong Wang[1*] and Qi Wu[6*]

Abstract

Background Spinal cord injury is followed by glial scar formation, which was long seen mainly as a physical barrier preventing axonal regeneration. Glial scar astrocytes lead to glial scar formation and produce inhibitory factors to prevent axons from growing through the scar, while inhibiting the conversion of reactive astrocytes into glial scar-forming astrocytes may represent an ideal treatment for CNS injury. Exercise is a non-invasive and effective therapeutic intervention for clinical rehabilitation of spinal cord injury. However, its precise therapeutic mechanisms still need to be continuously explored.

Methods 30 rats were randomly assigned to three groups (Sham, SCI, SCI + BWSTT; n = 10 rats per group). In this study, we employed the BBB scales and gait analysis system to examine the behavioral functions of the rats in each group. Furthermore, we utilized immunoblotting of spinal cord tissue at the injury site, in addition to histological staining and immunofluorescence staining, to explore glial scar aggregation and axonal regeneration in each group of rats.

Results Our results revealed that hindlimb motor function was significantly improved in SCI rats after a sustained subacute period of BWSTT, accompanied by the promotion of histological repair and nerve regeneration. Subsequent immunofluorescence staining and immunoblotting showed diminished astrocyte reactivity in the region surrounding the spinal cord injury as well as reduced expression and distribution of collagen fibers near the lesion after BWSTT. Additionally, a significant decrease in the expression of MMP-2/9, which is closely related to astrocyte migration, was observed in the vicinity of spinal cord tissue lesions.

Conclusion Our study demonstrates that a sustained BWSTT intervention during the subacute phase of spinal cord injury can effectively reduce astrocyte reactivity and glial scarring overgrowth, thereby facilitating functional recovery after SCI.

†Jili Cai, Yu Wang and Chenyuan Zhai are contributed equally to this work.

*Correspondence:
Tong Wang
wangtong60621@163.com
Qi Wu
wuqi87@126.com
Full list of author information is available at the end of the article

Keywords Spinal cord injury, Body weight-supported treadmill training, Glial scar, Astrocyte reactivity, Matrix metalloproteinase-2/9

Introduction

Spinal cord injury (SCI) represents a severe injury to the central nervous system (CNS) with associated complex complications and a relatively high disability rate [1]. The permanence of functional impairments can be attributed, at least in part, to the limited ability of injured CNS neurons to regenerate axons and re-establish functional connections [2]. This is due to a combination of factors, including the lack of intrinsic regeneration potential of neurons and the influence of extrinsic factors [3]. Glial scar is one of the prominent microenvironment inhibitors around the lesion site and is the major origin of the dysfunction of motor and sensory neurons after injury. The dynamic formation of glial scars primarily occurs during the subacute phase of SCI, within 7 to 14 days post-injury. However, the detrimental effects of overly aggregated dense scars may persist into the chronic phase and even remain permanently [4, 5]. Despite the implementation of a multitude of intervention strategies, it is regrettably the case that there are no effective treatments for preventing glial scar over formation at present.

Astrocytes constitute an important category of glial cells in the CNS. In response to SCI, astrocytes undergo characteristic phenotypic changes—known as reactive astrogliosis—that can exert beneficial or detrimental effects on the surrounding lesion microenvironment [6]. They proliferate and migrate to the injury site together with activated microglial cells, forming the glial component of the glial scar. Reactive astrocytes also physically ensnare fibroblasts by 7 days post-injury. The fibroblasts, in conjunction with the ECM components, contribute to the formation of the fibrotic component of the glial scar [5]. The activation and proliferation of astrocytes following a SCI results in the formation of glial scars [7]. The inhibition of the inflammatory phenotype astrocyte in SCI models has been observed to reduce the density of glial scars, thereby facilitating axon regeneration [8, 9]. Consequently, intervention of astrocytes may represent a potential therapeutic strategy for effectively controlling glial scars and promoting functional recovery from SCI.

Exercise has long been used as a therapy for SCI rehabilitation. It is an accessible, straightforward, and well-established therapy that can be implemented in a variety of clinical settings. The available evidence suggests that exercise-based rehabilitation following SCI can effectively reduce the expression of inflammatory factors at the site of injury [10]. Moreover, evidence indicates that exercise can inhibit the inflammatory activation of glial cells [11, 12]. Consequently, early exercise is likely to modulate the formation of glial scarring, thereby facilitating functional recovery. However, current research on post-SCI exercise interventions predominantly focuses on continuous protocols initiated during the subacute phase and extending into the chronic phase. While these studies have elucidated the sustained therapeutic benefits of long-term exercise training, the potential for early-stage positive effects emerging prior to chronic phase progression remains underexplored. It remains a critical question whether subacute-phase exercise interventions can induce measurable neuroprotective effects or enhance functional recovery prior to the maturation of chronic glial scars.

The objective of this study is to elucidate the therapeutic effects and the underlying mechanisms of exercise intervention during the subacute phase following injury. The results demonstrate that initiating an exercise intervention during the subacute phase may facilitate functional recovery following SCI, possibly by altering the reactivity of astrocytes at the site of injury to influence the formation of aggregated scar tissue. This study provides a theoretical foundation for the development of early exercise rehabilitation in clinical practice.

Materials and methods

Animals and SCI model

All experiments involving animals were approved by the Ethics Committee for Animal Experiments of Nanjing Medical University (license No. IACUC-2206045 and No. IACUC-2403019), Jiangsu Province, China. Female adult SPF 9-week-old Sprague–Dawley rats, approximately 210–250 g in weight, were obtained from the Animal Core Facility of Nanjing Medical University (Animal license: SYXK (Su) 2021–0023). The rats were housed in an environment with controlled conditions (temperature 22 ± 2 °C, and a 12/12-h light/dark cycle, 55 ± 5% relative humidity) with free access to food and water. They were allowed to acclimate to these conditions for at least one week prior to the commencement of the experiment.

The rats were randomly assigned to three groups (Sham, SCI, SCI + BWSTT; n = 10 rats per group) [13]. The SCI model was based on Allen's model [14, 15], which closely replicates the clinical presentation of bilateral lower limb paralysis following SCI. In brief, rats were anesthetized with an intraperitoneal injection of 1% (w/v)

pentobarbital sodium (50 mg/kg) in all surgeries. After removing the hair, a laminectomy was performed at T_{10}, the designated impact center. To ensure an optimal surgical field, the spinal cord was exposed approximately from T_9 to T_{11}. Subsequently, a spinal cord impactor with a 2.5 mm diameter tip (RWD, China) was utilized to induce a moderate incomplete SCI model, following a previously established protocol [16, 17], with an impact force of 250 kdyn. The presence of lower limb convulsion and localized hematoma of the injured spinal cord in rats indicated successful modeling. In the sham group, the exposed spinal cord was not compressed by the rod. At the conclusion of the surgical procedure, all rats were administered a single dose of penicillin potassium (32,000 U/100 g) via intramuscular injection. The bladders were manually emptied twice daily until spontaneous voiding was established.

Body weight-supported treadmill training

Prior to the surgical intervention (SCI), all rats underwent three days of treadmill training to facilitate adaptation. Body weight-supported treadmill training (BWSTT) prescription was based on the procedures of our previous study [18, 19]. The SCI + BWSTT group underwent body weight-supported treadmill training on the eighth day post-SCI, with treadmill speed at 6 m/min for a duration of 20 min, twice daily for a week. Prior to each treadmill training session, the bladder was manually massaged to facilitate emptying. The body weight support range was adjusted to approximately 30 ± 10%, providing a force of approximately 780N, depending on the hindlimb locomotor function of the rats during training. Specifically, the adjustment allowed the rats' backs to slightly arch while their hindlimbs gently lifted off the runway, enabling active participation in treadmill training.

Behavioral tests

The recovery of hindlimb motor function in rats was evaluated via the Basso-Beattie-Bresnahan (BBB) motor function scores [20]. Two independent examiners, who were blinded to the treatment groups, conducted the BBB test in an open field (1 m × 1 m). The scores ranged from 0 points (complete paraplegia) to 21 points (normal function). Hind limb joint mobility, hind limb coordination, and fine paw movements were assessed. Each group (n = 10 rats per group) was evaluated the day before surgery and daily after SCI at the regular time.

Gait analysis was conducted for each group (n = 10 rats per group) of rats using a CatWalk XT® automated quantitative gait analysis system (Noldus, Wageningen, Netherlands) 14 days after SCI. All rats were recorded for at least three consecutive walking cycles. Before detection, the appropriate position of the camera and the detection parameters were set, and the width and length of the runway were adjusted. The test was carried out in a dark and quiet environment. After detection, each animal's footprints were manually marked, and the gait parameters were automatically calculated by the system. The mean values of the gait parameters of both hind limbs of each group of rats were statistically analyzed, including regularity index, mean intensity, duty cycle, stride length, print area and average speed. To prevent the influence of body weight on gait parameters, the parameters were corrected (hindlimb/forelimb, H/F) according to the previously described methodology [21], including the two parameters more related to animal weight, mean intensity and print area.

Tissue collection

On day 14 post-SCI, all rats were euthanized with sodium pentobarbital (100 mg/kg) to ensure animal welfare and minimize discomfort. The T_9–T_{11} spinal cord tissue (within a 0.5 cm range centered around the impact site) was harvested for biochemical analysis. For tissue staining, longitudinal sections (n = 3) were prepared from the dorsal side of the spinal cord (on the impacted side, with the impact site as the center) to the region near the central canal. Continuous sections were obtained, and efforts were made to ensure uniformity by slicing at the same height across all groups throughout the experimental process. For transverse sections (n = 3), continuous tissue slices were collected from a 0.5 cm region centered around the impact site, ensuring that sections from all groups were taken at the same height to maintain consistency.

Immunofluorescence staining

For immunofluorescence staining, the tissue was stored in 4% paraformaldehyde for 24 h at 4 °C. Thereafter, the tissues were dehydrated, made transparent, dipped in wax, embedded, and sliced into 5 μm-thick serial sections using a microtome (RM2245, Leica, German). The spinal cord sections were deparaffinized by sequential incubation in xylene, anhydrous ethanol, 95% ethanol, 85% ethanol, and 75% ethanol. Following a wash in distilled water, the sections were subjected to antigen retrieval by microwave treatment in citric acid antigen retrieval buffer (pH 6.0). Subsequently, the sections were incubated for one hour at room temperature in phosphate-buffered saline (PBS) containing 10% donkey serum albumin and 0.3% Triton X-100. Following this, the sections were washed in PBS and incubated overnight at 4 °C with primary antibodies. The primary antibodies utilized for immunofluorescence were mouse anti-GFAP (1:500, ab279289, Abcam, USA), anti-NeuN (1:400, 94403, CST, USA) and anti-NF-H/NF200 (1:200,

18934-1-AP, Proteintech, China). Following three washes with PBS for five minutes each, the corresponding secondary antibodies, Alexa Fluor 594 (red) or Alexa Fluor 488 (green), were added in the dark. The samples were then incubated at room temperature for two hours, after which they were washed three times with PBS for five minutes each. Finally, an antifade mounting medium with DAPI (P0131, Beyotime, China) was added for sealing and preservation at 4 °C. Representative images were captured using the Zeiss LSM 800 confocal microscope, and the fluorescence intensity was analyzed using ImageJ software (NIH, USA).

H&E staining, Masson's trichrome staining and Sirius red staining

In brief, the sections were stained with hematoxylin and eosin (H&E) in accordance with the supplier's specifications for H&E staining (C0105, Beyotime, China). For Masson staining, the longitudinal sections were stained with Masson's Trichrome Staining Kit (C0189, Beyotime, China). For Sirius red staining [22], the tissue sections were incubated with a solution of Sirius red stain (BL1270A, Biosharp, China). Finally, the sections were mounted in synthetic resin. The sections were photographed using a LEICA DM2500 microscope. The quantification of the lesion area was conducted with the thresholding method in Image J software.

Western blot analysis

Total protein was extracted from the tissue samples using radioimmunoprecipitation assay lysis buffer (P0013B, Beyotime, China), which contained a protease inhibitor and phosphatase inhibitor cocktail (P1082, Beyotime, China). The supernatants of the tissue lysates were then collected by centrifugation at 12,000 g for 15 min at 4 °C. Protein concentration was quantified using the bicinchoninic acid protein assay (23225, Thermo, USA). A total of 20 μg of protein was resolved by sodium dodecyl sulfate–polyacrylamide gel electrophoresis and transferred to polyvinylidene difluoride membranes (Millipore, Billerica, MA, USA). The membranes were blocked with 5% milk at room temperature for 2 h, and then incubated overnight with primary antibody at 4 °C. The primary antibodies used were as follows: (MMP-2, MMP-9, collagen I, vimentin). Following a washing step with TBST, the membranes were incubated with horseradish peroxidase-conjugated secondary antibodies for a period of two hours at room temperature. Signals were detected by the Tanon-5200 Multi Gel Imaging Analysis System (Tanon, China), and ImageJ was used for quantitative analysis.

Statistical analysis

The data are presented as the mean ± standard error of the mean (SEM). Normally distributed multiple time-point measurements between multiple groups such as BBB scores were analyzed by two-way analysis of variance (ANOVA). Multiple-group comparisons were statistically analyzed with one-way ANOVA followed by the Tukey method or nonparametric tests using Prism 10.1.1 software (GraphPad Software Inc., US). A value of $p < 0.05$ was considered significant.

Results

BWSTT promotes the recovery of motor function after SCI

To evaluate the therapeutic effect of BWSTT on functional recovery after SCI, we assessed hindlimb motor function in rats on each day after injury using the BBB scores and examined gait function in rats in each group on day 14 after injury (Fig. 1A). On the first day after the injury, the hindlimbs of all rats were completely paralyzed (BBB score < 1). Thereafter, the rats demonstrated varying extents of recovery. It was unexpected that rats treated with the BWSTT exhibited a higher BBB score ($p < 0.05$) than untreated rats with SCI on day 13 and day 14 after SCI (Fig. 1B). Subsequent gait analysis results provide a more detailed and comprehensive visualization of the facilitating effect of the BWSTT on the recovery of motor function (Fig. 1C–J). The most obvious performance is that on the 14th day of spinal cord injury, the bilateral hindlimb footprints of SCI group rats cannot be detected, while those of the SCI + BWSTT group can be partially detected. The results demonstrated that the SCI + BWSTT group exhibited evidence of hindlimb support during a complete walking cycle and displayed enhanced coordination and organization throughout the walk in comparison to the SCI group (Fig. 1C and G). A statistical analysis of the gait function parameters indicated that the SCI + BWSTT group exhibited statistically significant improvements ($p < 0.05$) in multiple key metrics when compared to the SCI group, including regularity index, mean intensity, duty cycle, stride length, and footprints area (Fig. 1D–F and H–I). However, there was no statistically significant ($p > 0.05$) enhancement in average speed between the SCI + BWSTT group and the SCI group (Fig. 1J). These results reflected that BWSTT during the subacute phase of SCI can significantly promote the motor function recovery of SCI rats.

BWSTT promotes histological repair of the damaged spinal cord

Then we investigate the effect of BWSTT on the structural repair of injured spinal cord tissue. The histological changes in the injured spinal cord at two weeks

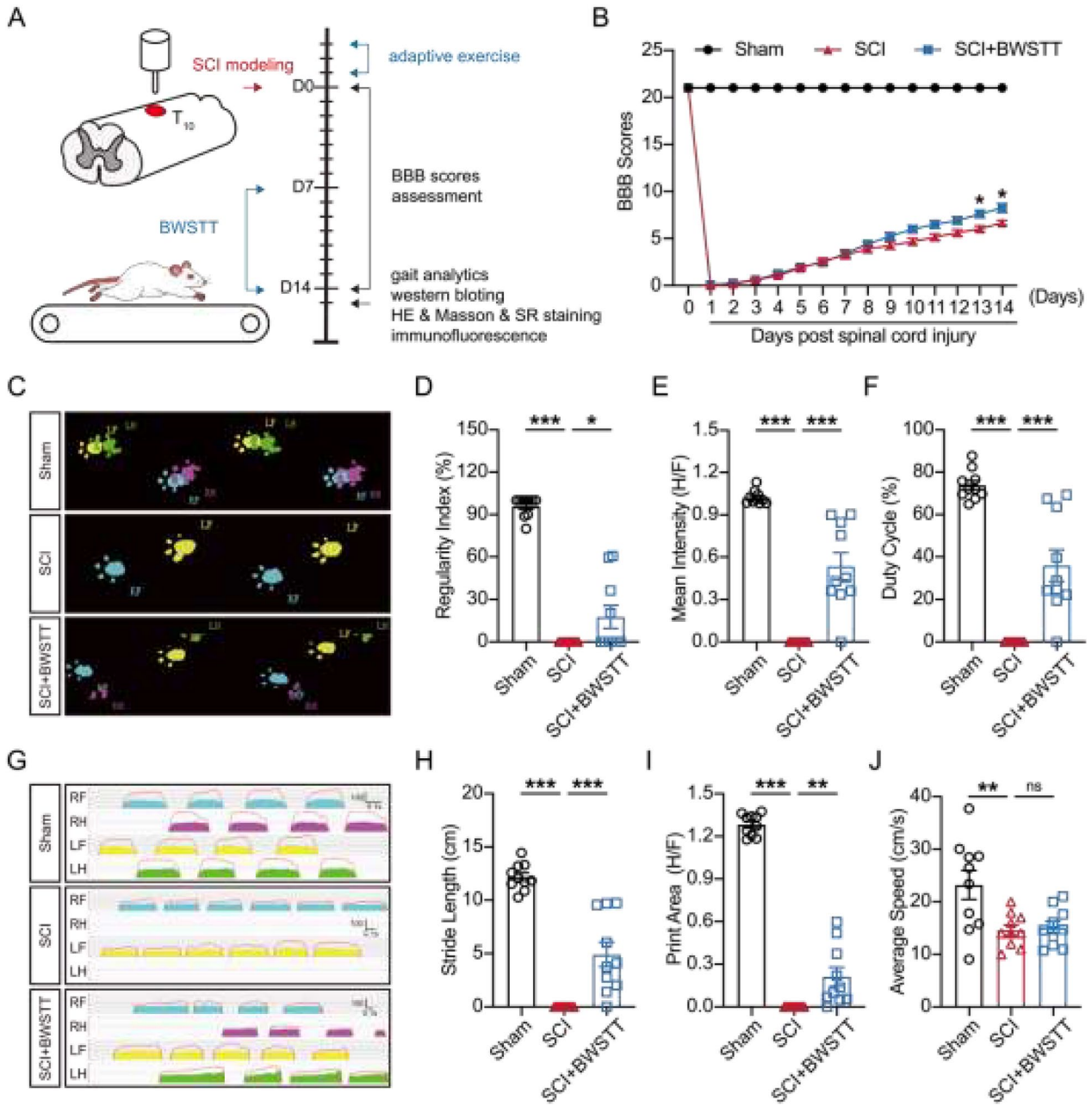

Fig.1 BWSTT improved functional recovery after SCI. **A** Time-line diagram of spinal cord injury, BWSTT treatment, and experimental analysis in rats. **B** The BBB scores in each group (n = 10). **C**–**J** The CatWalk XT® automated gait analysis results in each group (n = 10). The representative images of footprint intensity during a pedestrian cycle **C** and footprint pressure–time chart **G** in each group. The quantification analysis of the CatWalk of gait analysis parameters in each group, **D** regularity index, **E** mean intensity (H/F), **F** duty cycle, **H** stride length, **I** print area, **J** average speed. Values are expressed as the mean ± s.e.m, $\star p < 0.05$, $\star\star p < 0.01$, and $\star\star\star p < 0.001$, as determined by one-way ANOVA. RF-right forelimb, RH-right hindlimb, LF-left forelimb, LH-left hindlimb

post-injury were evaluated using H&E staining and Masson staining (Fig. 2A, B). The longitudinal H&E staining results demonstrated that the SCI group exhibited severe tissue damage and a considerable infiltration of inflammatory cells, with a notable reduction ($p < 0.05$) in the injured area following SCI in the SCI + BWSTT group (Fig. 2C). Moreover, the results of the Masson staining demonstrated a significantly lower average percentage of fibrosis ($p < 0.05$) in the SCI + BWSTT group in comparison to the SCI group, particularly in the core of the injury

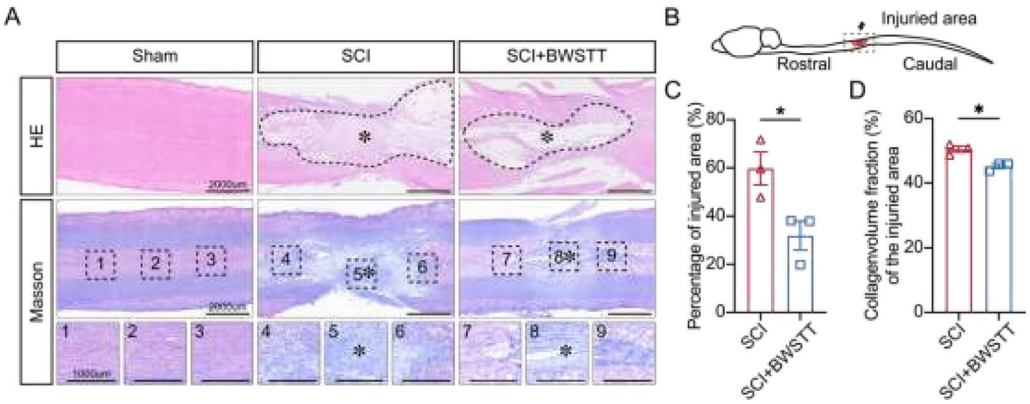

Fig. 2 BWSTT promotes histological repair of the damaged spinal cord. **A** Representative H&E staining and Masson staining images in longitudinal sections of the spinal cord from each group (n = 3). The line labels the injured area and * Indicates the lesion center. Scale bar = 2000 μm, 1000 μm. **B** The schematic representation of the injury site is utilized for pathological staining. **C**, **D** Quantification analysis of the injured area percentage of the H&E staining (**C**) and collagen volume fraction of the Masson staining (**D**). Values are expressed as the mean ± s.e.m, * p < 0.05 as determined by one-way ANOVA

(Fig. 2D). These results indicated that BWSTT during the subacute phase of spinal cord injury promotes histological repair of the damaged spinal cord.

BWSTT promotes axonal regeneration after SCI

Massive neuronal cell death and failure of axonal regeneration can lead to long-term structural and functional damage. We subsequently employed immunofluorescence staining to assess the effects of BWSTT during the subacute phase of SCI on neuronal survival and axonal regeneration. The survival of neurons in the vicinity of the lesion site was visualized by NeuN immunofluorescence staining of spinal cord sections obtained on the 15th day (Fig. 3A). The results demonstrated a notable reduction in the number of $NeuN^+$ cells in the SCI group when compared to the Sham group. However, the NeuN-positive area was significantly higher ($p < 0.05$) in the SCI + BWSTT group than in the SCI group (Fig. 3B). Additionally, an increase in NF200 + area was observed following BWSTT treatment ($p < 0.05$) when compared to the SCI group (Fig. 3C, D). These data indicate that BWSTT intervention during the sustained subacute phase may somewhat promote retention of peri-lesional neurons. It is noteworthy that the data also indicated the emergence of additional $NF200^+$ regions in the core of the lesion, suggesting that BWSTT may have facilitated axonal reattachment and regeneration across the scar.

BWSTT reduces astrocyte reactivity and glial scar formation

To ascertain whether BWSTT reduces glial scar aggregating and affects astrocyte reactivity at the injury border, as proposed by Escartin et al., we examined the molecular markers and functional readouts in vivo [23, 24]. The results demonstrated a notable reduction ($p < 0.05$) in the number of GFAP-positive areas at the injury border in the SCI + BWSTT group when compared to the SCI group. Furthermore, astrocytes in the vicinity of the border demonstrated a reduced propensity to undergo morphological alterations, such as hypertrophy of shape and thickening of branches, which are commonly associated with reactive astrocytes (Fig. 4A–C). Similarly, the western blotting results supported the reduction in the expression of Vimentin ($p < 0.05$) after the BWSTT intervention (Fig. 4D and F). Prior research has indicated that deficiencies in GFAP and waveform proteins are linked to augmented axonal plasticity and superior functional recovery following SCI. This phenomenon may be linked to a reduction in astrocyte reactivity [23, 25, 26]. Therefore, the results of our experiments suggest that the efficacy of BWSTT in the subacute period may be attributed to its capacity to diminish the astrocyte reactivity in proximity to the lesion site. Moreover, the interaction between reactive astrocytes and type 1 fibronectin results in the formation of scar-forming astrocytes [27, 28]. Consequently, we investigated the protein expression and distribution of collagen fibers in the vicinity of the lesions (Fig. 4D and G). The results revealed a markedly diminished deposition of collagen ($p < 0.05$) and a decline in the expression of collagen I in the vicinity of the lesions

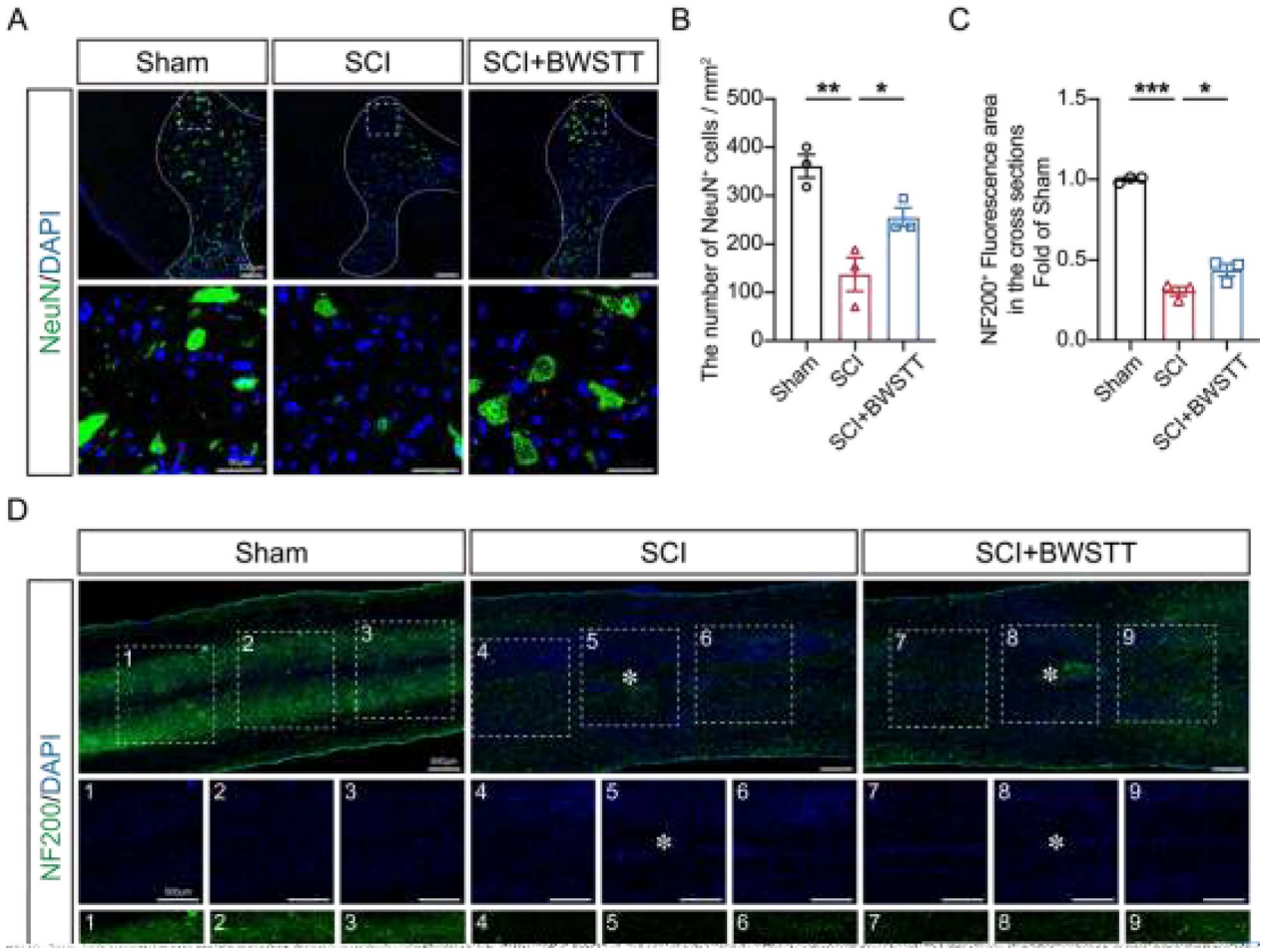

Fig. 3 BWSTT inhibits neuronal cell death and promotes axonal regeneration after SCI. **A** Representative immunofluorescence images of NeuN (a neuronal marker) (green) from the anterior horn area of the spinal cord (transverse sections of the caudal region of the injured spinal cord) in each group following SCI (n = 3). Nuclei were counterstained with DAPI (blue). Scale bar = 100 μm, 50 μm. **B**, **C** Quantification of the number of $NeuN^+$ cells/mm^2 in (**A**) and $NF200^+$ fluorescence intensity area in (**D**). **D** Representative immunofluorescence images of NF200 (key components of the neuronal cytoskeleton) (green) and DAPI (blue) in longitudinal sections of the spinal cord from each group after SCI (n = 3). Scale bar = 500 μm and * Indicates lesion center. Values are expressed as the mean ± s.e.m, * $p < 0.05$, ** $p < 0.01$, and *** $p < 0.001$, as determined by one-way ANOVA

($p < 0.05$) within the SCI + BWSTT cohort when compared to the SCI group (Fig. 4H).

BWSTT downregulates the matrix metalloproteinase-2/9 after SCI

To investigate the mechanism of inhibition of glial scar by BWSTT, we investigated MMP-2/9 protein expression in the epicenter at 15 d after SCI (Fig. 5A). Compared with the Sham group, MMP-2/9 expression increased significantly after SCI ($p < 0.05$). Furthermore, BWSTT significantly upregulated MMP-2/9 expression ($p < 0.05$) compared to that in rats that received SCI alone (Fig. 5B, C). The results of this study are comparable to those reported in the study conducted by Ying et al., although the timing and methodology of our intervention differed [29]. These data indicated that BWSTT downregulates the MMP-2/9 after SCI.

Discussion

This study demonstrates that the utilization of BWSTT during the subacute phase can effectively facilitate the recuperation of neuromotor function after SCI. It was determined that this therapeutic effect was, at least in part, due to the effectiveness of BWSTT in reducing astrocyte reactivity and the expression of MMP-2/9 around the lesion during the formation of glial scarring. Previous studies on the therapeutic effects of exercise rehabilitation after SCI have concentrated on the chronic phase [30]. This study, however, focuses on the subacute phase, which is the most crucial period for scar formation

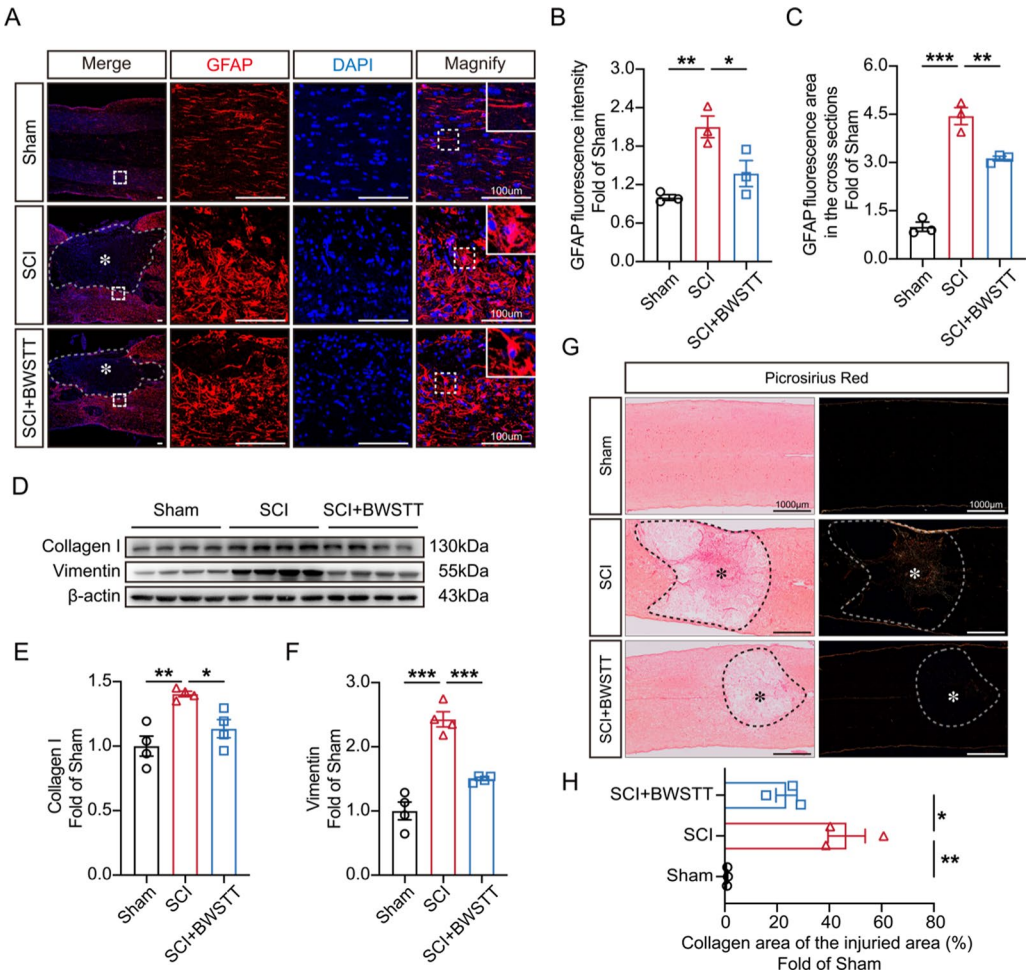

Fig. 4 BWSTT reduces the astrocyte reactivity and the expression of collagen I. **A** Representative immunofluorescence images of GFAP (red) and DAPI (blue) of the injured site in longitudinal sections of the spinal cord form each group (n = 3). Scale bar = 100 μm, and * Indicates the lesion center. **B**, **C** Quantification analysis of the GFAP fluorescence intensity **B** and the GFAP$^+$ fluorescence area in the cross sections in each group. **D**–**F** Representative images of Western blotting and quantification analysis of collagen I, vimentin, and β-actin in each group (n = 4). **G** Representative images of Picrosirius Red staining in longitudinal sections of the spinal cord form each group (n = 3). Scale bar = 1000 μm, and * Indicates the lesion center. **H** Quantification analysis of the collagen area of the injured site in (**G**). Values are expressed as the mean ± s.e.m, *$p < 0.05$, **$p < 0.01$, and ***$p < 0.001$, as determined by one-way ANOVA

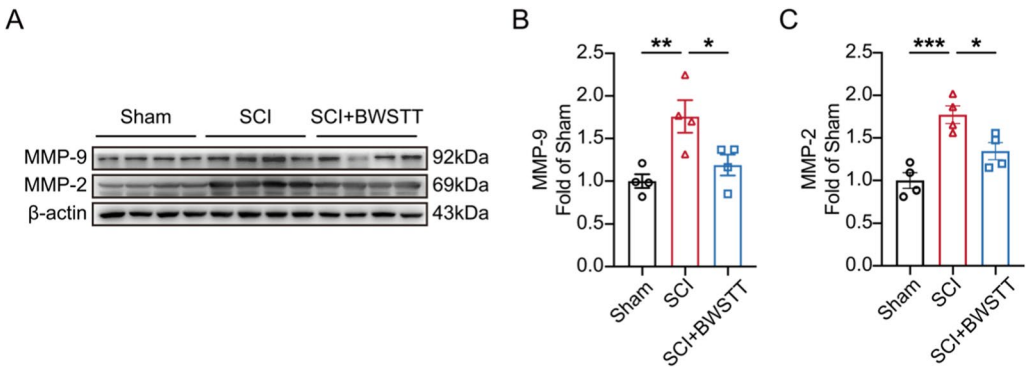

Fig. 5 BWSTT downregulates the Matrix Metalloproteinase-2/9(MMP-2/9) after SCI. **A** Representative images of Western blotting of MMP-9, MMP-2, and β-actin in each group after SCI (n = 4). **B**, **C** Quantification analysis of MMP-9 (**B**) and MMP-2 (**C**) relative protein expression in the epicenter. Values are expressed as the mean ± s.e.m, *$p < 0.05$, **$p < 0.01$, and ***$p < 0.001$, as determined by one-way ANOVA

following a SCI. The aim is to investigate the impact of exercise training on the process of scar formation after SCI, with the objective of providing a theoretical foundation for advancing clinical exercise rehabilitation in the early stages of injury.

The decision to employ exercise therapy as an intervention was informed by the extensive research conducted by our group over time [18, 19, 31]. Moreover, in both preclinical and clinical practice [32–37], exercise therapy has been demonstrated to facilitate functional recovery after SCI as a non-invasive, non-pharmacological intervention. However, the existing studies have predominantly concentrated on the long-term therapeutic effects of exercise, which typically persist for several weeks [38, 39]. In contrast, studies on the early therapeutic effects of exercise are scarce. Some studies have demonstrated that early exercise intervention can effectively promote the recovery of neuromotor function after SCI, with aquatic treadmill training being an effective method [12, 29]. However, in consideration of the potential timing of clinical exercise rehabilitation intervention and the time window for glial scar formation and maturation, we elected to conduct the exercise intervention in the subacute phase of SCI and incorporated a weight reduction device to address the issue of diminished treadmill exercise efficacy due to hindlimb paralysis in rats. BWSTT can effectively simulate existing clinical rehabilitation interventions while facing fewer limitations in the early rehabilitation process. Additionally, our previous work [18, 19], along with the studies by Xu [40] and Singh [41], has demonstrated that BWSTT intervention effectively promotes functional recovery after SCI. Our results indicate that, following BWSTT intervention, the SCI + BWSTT group showed better functional recovery compared to the SCI group, including higher BBB scores and an earlier onset of bilateral hindlimb support during walking. However, no improvement was observed in the average speed parameter. The limited duration of the exercise intervention may have contributed to this outcome. It is possible that while the earlier emergence of bilateral hindlimb support was observed, this change was not sufficient to significantly affect walking speed throughout the intervention period.

Exercise typically yields mild, systemic therapeutic effects, which extend to positive outcomes at the injury site. In traumatic brain injury models, Barrett et al. [42] demonstrated that exercise can modulate local neuroinflammation and enhance neuroplasticity, thereby partially restoring hippocampal homeostasis. Similarly, Amorós-Aguilar et al. [43] reported that early exercise mitigates microglial activation and neuronal loss in the hippocampus. In the present study, our results indicate that BWSTT intervention also exerted a positive effect on spinal cord tissue at the injury site. A greater portion of the spinal cord tissue surrounding the injury was preserved, with more $NeuN^+$ and $NF200^+$ regions observed at the injury site. Previous studies have confirmed the positive effects of exercise interventions on promoting axonal regeneration and facilitating motor function recovery in individuals with SCI [44, 45]. Based on these findings, although we did not conduct a more in-depth analysis of neuronal survival at the injury site, our results, in conjunction with similar findings from Yang et al. [12], suggest that BWSTT may positively influence the preservation of neurons and axons at the injury site following SCI.

Glial scarring is a key event in the remodeling of the microenvironment during the subacute phase, consisting of both molecular and cellular components. Our results suggest that BWSTT reduces inhibitory molecules, such as collagen I and vimentin, around the injury site. Additionally, BWSTT intervention attenuated reactive astrogliosis [23, 46], as evidenced by reduced hypertrophic changes, diminished extension of branches, and downregulated $GFAP^+$ area in astrocytes at the lesion site. Furthermore, we also found that BWSTT significantly reduced the area of collagen volume fraction in SCI rats by using Masson staining, which is commonly used to assess fibrotic areas within glial scars. All of these data, although indirect, is sufficient to demonstrate the effect of treadmill training (BWSTT) on reducing excessive scarring (glial scarring). There are currently two opposing perspectives on glial scarring following SCI. Some studies suggest that glial scars can limit the spread of cytotoxic molecules and help stabilize the propagation of secondary injury [47, 48]. In contrast, excessive accumulation of scar tissue forms a persistent physical and chemical barrier that obstructs axonal regeneration through both mechanical blockade and chemical inhibition, ultimately hindering functional recovery [49, 50]. In our study, BWSTT intervention led to greater tissue preservation and less deposition of inhibitory molecules. A reasonable explanation for this is that the effect of BWSTT on glial scarring is 'mild'—it does not cause excessive tissue damage due to a lack of glial scar formation, nor does it result in excessive scar accumulation that obstructs subsequent axonal regeneration. However, this explanation requires further validation through additional studies.

Matrix metalloproteinase (MMP) activation plays a critical role in migration, inflammation, and scar formation, which contribute to neurological disability. Previous studies have shown that MMP-2 and MMP-9, key members of the MMP family, are crucial in scar formation after SCI. These enzymes degrade inhibitory molecules associated with glial scars [51–53], and facilitate the migration of cellular components [54–56], including

astrocytes and fibroblasts. Our results demonstrate that BWSTT, administered during the sustained subacute phase, effectively downregulates MMP-2/9 expression around the injured area, in line with previously reported findings [29]. Hsu et al. observed a significant reduction in serotonergic axons caudal to the lesion in SCI mice lacking MMP-2 at 42 days post-injury, accompanied by extensive glial scarring [57]. In contrast, our study indicates that the downregulation of MMP-2/9 expression by BWSTT intervention promotes functional recovery in SCI rats and reduces the excessive formation of glial scarring. This may be because MMP-2 deficiency triggers a compensatory increase in MMP-9 expression, which enhances inflammatory cell infiltration and contributes to excessive scar formation [56]. While MMP-2 deficiency may have a beneficial effect in reducing scar formation during the subacute phase, it does not appear to sufficiently offset the negative consequences of the compensatory increase in MMP-9 expression.

In addition to modulating astrocyte migration, the therapeutic effects of exercise may also be associated with influencing the fate of reactive astrocytes [58]. The prevailing view among researchers is that reactive astrocytes can exert a dual effect [59]. However, the excessive aggregation of scar-forming astrocytes around the injured tissue is generally considered detrimental to axonal regeneration and functional recovery. Studies have shown that reactive astrocytes can gradually transition into scar-forming astrocytes via the type 1 collagen integrin-N-cadherin axis, highlighting the environment-dependent plasticity of reactive astrogliosis [28]. Our results demonstrate that following BWSTT intervention, there was a significant reduction in the number of reactive astrocytes around the injury site and in the expression of local ECM molecules, including vimentin and collagen I. Moreover, the SCI + BWSTT group showed improved axonal survival at the injury site compared to the SCI group. It is reasonable to suggest that the therapeutic effect of exercise is mediated through the remodeling of the microenvironment, reducing the emergence and persistence of excessive reactive and scar-forming astrocytes. Recent research has revealed that glial scarring persists into the chronic phase, with scar-forming astrocytes playing a crucial role in its maintenance [60]. This hypothesis provides valuable insights into the mechanisms underlying the efficacy of long-term exercise interventions in inhibiting scar tissue accumulation and promoting axonal regeneration during the chronic phase.

The main limitation of this study is the absence of detection of astrocyte subtypes. While the initial findings suggest that BWSTT reduces reactive astrocytes, thereby inhibiting the formation of aggregated scar tissue and promoting functional recovery, the phenotypic changes in astrocytes, especially those involved in scar formation, were not assessed. Although collagen expression and GFAP morphology were analyzed, the study did not examine the alterations in the astrocytic phenotype following the exercise intervention. Therefore, future studies should focus on investigating how BWSTT influences these phenotypic changes in astrocytes. Additionally, glial scarring after SCI forms both a physical and chemical barrier, but this study did not evaluate the effects of BWSTT on local inhibitory molecules, such as CSPGs, through additional staining. While the findings suggest that BWSTT may have neuroprotective effects through enhanced neuronal survival at the lesion site, the absence of direct mechanistic validation precludes definitive conclusions regarding this proposed pathway. Finally, while various cellular components and substances contribute to scar formation, the current study primarily addresses the effects of exercise on astrocytes. Future research could benefit from exploring other cellular components involved in the scarring process.

Conclusions

In conclusion, the present study reveals that BWSTT during the subacute phase maybe effectively inhibit glial scar overgrowth by decreasing the reactivity of astrocytes to promote the recovery of SCI function, which may be realized through the downregulation of MMP-2/9. This study demonstrated that BWSTT during the subacute phase is an effective strategy for promoting motor function recovery in SCI rats and provides a theoretical basis for clinical exercise to promote SCI functional recovery.

Abbreviations

ANOVA	Analysis of variance
BBB	Basso-Beattie-Bresnahan
BWSTT	Body weight-supported treadmill training
CNS	Central nervous system
CSPGs	Chondroitin sulfate proteoglycans
DAPI	4′,6-Diamidino-2-phenylindole
ECM	Extracellular matrix
GFAP	Glial fibrillary acidic protein
H&E	Hematoxylin and eosin
MMP-2/9	Matrix Metalloproteinase-2/9
NF200	200 KDa neurofilament protein
PBS	Phosphate-buffered saline
SCI	Spinal cord injury
SEM	Standard error of the mean

Supplementary Information

The online version contains supplementary material available at https://doi.org/10.1186/s12868-025-00947-7.

Supplementary Material 1.

Acknowledgements

Not applicable.

Author contributions
Jili Cai: Writing – original draft, Visualization, Methodology, Formal analysis, Data curation, Conceptualization. Yu Wang: Visualization, Project administration, Software. Chenyuan Zhai: Visualization, Methodology, Validation, Supervision, Data curation. Kunmao Jiang: Software, Methodology. Zun Wang: Methodology, Project administration. Lu Fang: Validation, Investigation, Data curation. Xiangzhe Li: Validation, Supervision, Software. Wentao Liu:Supervision, Methodology. Tong Wang: Writing – review & editing, Supervision, Resources, Funding acquisition. Qi Wu: Writing – review & editing, Supervision, Resources, Investigation, Conceptualization. Jili Cai, Yu Wang, Chenyuan Zhai are contributed equally to this work. Corresponding author: Wang Tong; Wu Qi.

Funding
This work was supported by grants from the National Natural Science Foundation of China (82302877, 82172541) and Hunan Provincial Natural Science Foundation (2023JJ30549).

Availability of data and materials
All statistical results are stated in the article, and raw data are available from the corresponding author on reasonable request.

Declarations

Ethics approval and consent to participate
All experiments involving animals were approved by the Ethics Committee for Animal Experiments of Nanjing Medical University (license No. IACUC-2206045 and No. IACUC-2403019), Jiangsu Province, China.

Consent for publication
Not applicable.

Competing interests
The authors declare no competing interests.

Author details
[1]Rehabilitation Medicine Center, The First Affiliated Hospital of Nanjing Medical University, Nanjing 210029, China. [2]Department of Rehabilitation, Suzhou Hospital, Nanjing Medical University, Suzhou 215008, China. [3]Jiangsu Key Laboratory of Neurodegeneration, Department of Pharmacology, Nanjing Medical University, Nanjing 211166, Jiangsu, China. [4]Rehabilitation Medicine Department, School of Acupuncture and Tuina, School of Health and Rehabilitation, Nanjing University of Chinese Medicine, Nanjing 210023, China. [5]Rehabilitation Medicine Center, Suzhou Hospital, Affiliated Hospital of Medical School, Nanjing University, Suzhou 215153, Jiangsu, China. [6]Department of Rehabilitation, Hengyang Medical School, The First Affiliated Hospital, University of South China, Hengyang, Hunan, China.

Received: 9 November 2024 Accepted: 21 March 2025
Published online: 28 April 2025

References

1. Crispo JAG, Kuramoto LK, Cragg JJ. Global burden of spinal cord injury: future directions. Lancet Neurol. 2023;22:976–8.
2. Zheng B, Tuszynski MH. Regulation of axonal regeneration after mammalian spinal cord injury. Nat Rev Mol Cell Biol. 2023;24:396–413.
3. Gong L, Gu Y, Han X, Luan C, Liu C, Wang X, et al. Spatiotemporal dynamics of the molecular expression pattern and intercellular interactions in the glial scar response to spinal cord injury. Neurosci Bull. 2023;39:213–44.
4. Lima R, Monteiro A, Salgado AJ, Monteiro S, Silva NA. Pathophysiology and therapeutic approaches for spinal cord injury. Int J Mol Sci. 2022;23:13833.
5. Clifford T, Finkel Z, Rodriguez B, Joseph A, Cai L. Current advancements in spinal cord injury research—glial scar formation and neural regeneration. Cells. 2023;12:853.
6. Vangansewinkel T, Lemmens S, Tiane A, Geurts N, Dooley D, Vanmierlo T, et al. Therapeutic administration of mouse mast cell protease 6 improves functional recovery after traumatic spinal cord injury in mice by promoting remyelination and reducing glial scar formation. FASEB J. 2023;37:e22939.
7. Chen X, Chen C, Hao J, Zhang J, Zhang F. Effect of CLIP3 upregulation on astrocyte proliferation and subsequent glial scar formation in the rat spinal cord via STAT3 pathway after injury. J Mol Neurosci. 2018;64:117–28.
8. Yang T, Xing L, Yu W, Cai Y, Cui S, Chen G. Astrocytic reprogramming combined with rehabilitation strategy improves recovery from spinal cord injury. FASEB J. 2020;34:15504–15.
9. Liu A, Yu L, Li X, Zhang K, Zhang W, So K, et al. Celsr2-mediated morphological polarization and functional phenotype of reactive astrocytes in neural repair. Glia. 2023;71:1985–2004.
10. Walsh CM, Gull K, Dooley D. Motor rehabilitation as a therapeutic tool for spinal cord injury: new perspectives in immunomodulation. Cytokine Growth Factor Rev. 2023;69:80–9.
11. Mu L, Xia D, Cai J, Gu B, Liu X, Friedman V, et al. Treadmill exercise reduces neuroinflammation, glial cell activation and improves synaptic transmission in the prefrontal cortex in 3 × Tg-AD mice. Int J Mol Sci. 2022;23:12655.
12. Ying X, Yu X, Zhu J, Li X, Zheng Y, Xie Q, et al. Water treadmill training ameliorates neurite outgrowth inhibition associated with NGR/RhoA/ROCK by inhibiting astrocyte activation following spinal cord injury. Oxid Med Cell Longev. 2022;2022:1–20.
13. Jung S-Y, Seo T-B, Kim D-Y. Treadmill exercise facilitates recovery of locomotor function through axonal regeneration following spinal cord injury in rats. J Exerc Rehabil. 2016;12:284–92.
14. Zhang N, Fang M, Chen H, Gou F, Ding M. Evaluation of spinal cord injury animal models. Neural Regen Res. 2014;9:2008–12.
15. Basso DM, Beattie MS, Bresnahan JC. graded histological and locomotor outcomes after spinal cord contusion using the NYU weight-drop device versus transection. Exp Neurol. 1996;139:244–56.
16. Verma R, Virdi JK, Singh N, Jaggi AS. Animals models of spinal cord contusion injury. Korean J Pain. 2019;32:12–21.
17. Zhai C, Wang Z, Cai J, Fang L, Li X, Jiang K, et al. Repeated trans-spinal magnetic stimulation promotes microglial phagocytosis of myelin debris after spinal cord injury through LRP-1. Exp Neurol. 2024;379: 114844.
18. Li X, Wu Q, Xie C, Wang C, Wang Q, Dong C, et al. Blocking of BDNF-TrkB signaling inhibits the promotion effect of neurological function recovery after treadmill training in rats with spinal cord injury. Spinal Cord. 2019;57:65–74.
19. Li X, Song X, Fang L, Ding J, Qi L, Wang Q, et al. Body weight-supported treadmill training ameliorates motoneuronal hyperexcitability by increasing GAD-65/67 and KCC2 expression via TrkB signaling in rats with incomplete spinal cord injury. Neurochem Res. 2022;47:1679–91.
20. Basso DM, Beattie MS, Bresnahan JC. A sensitive and reliable locomotor rating scale for open field testing in rats. J Neurotrauma. 1995;12:1–21.
21. Zheng G, Zhang H, Tail M, Wang H, Walter J, Skutella T, et al. Assessment of hindlimb motor recovery after severe thoracic spinal cord injury in rats: classification of CatWalk XT® gait analysis parameters. Neural Regen Res. 2023;18:1084.
22. Huang Y, Gao P, Qin T, Chu B, Xu T, Yi J, et al. Delayed inhibition of collagen deposition by targeting bone morphogenetic protein 1 promotes recover. Matrix Biol. 2023;118:69–91.
23. Escartin C, Galea E, Lakatos A, O'Callaghan JP, Petzold GC, Serrano-Pozo A, et al. Reactive astrocyte nomenclature, definitions, and future directions. Nat Neurosci. 2021;24:312–25.
24. Wanner IB, Anderson MA, Song B, Levine J, Fernandez A, Gray-Thompson Z, et al. Glial scar borders are formed by newly proliferated, elongated astrocytes that interact to corral inflammatory and fibrotic cells via STAT3-dependent mechanisms after spinal cord injury. J Neurosci. 2013;33:12870–86.
25. Chen K-Z, Liu S-X, Li Y-W, He T, Zhao J, Wang T, et al. Vimentin as a potential target for diverse nervous system diseases. Neural Regen Res. 2023;18:969.
26. Menet V, Prieto M, Privat A, Ribotta MGY. Axonal plasticity and functional recovery after spinal cord injury in mice deficient in both glial fibrillary acidic protein and vimentin genes. Proc Natl Acad Sci USA. 2003;100:8999–9004.
27. Okada S, Hara M, Kobayakawa K, Matsumoto Y, Nakashima Y. Astrocyte reactivity and astrogliosis after spinal cord injury. Neurosci Res. 2018;126:39–43.

28. Hara M, Kobayakawa K, Ohkawa Y, Kumamaru H, Yokota K, Saito T, et al. Interaction of reactive astrocytes with type I collagen induces astrocytic scar formation through the integrin–N-cadherin pathway after spinal cord injury. Nat Med. 2017;23:818–28.
29. Ying X, Xie Q, Li S, Yu X, Zhou K, Yue J, et al. Water treadmill training attenuates blood-spinal cord barrier disruption in rats by promoting angiogenesis and inhibiting matrix metalloproteinase-2/9 expression following spinal cord injury. Fluids Barriers CNS. 2020;17:70.
30. Neckel ND, Dai H. Viscous field training induces after effects but hinders recovery of overground locomotion following spinal cord injury in rats. Behav Brain Res. 2021;412: 113415.
31. Wu Q, Cao Y, Dong C, Wang H, Wang Q, Tong W, et al. Neuromuscular interaction is required for neurotrophins-mediated locomotor recovery following treadmill training in rat spinal cord injury. PeerJ. 2016;4: e2025.
32. Wu M, Kim J, Wei F. Facilitating weight shifting during treadmill training improves walking function in humans with spinal cord injury: a randomized controlled pilot Study. Am J Phys Med Rehabil. 2018;97:585–92.
33. Duan R, Qu M, Yuan Y, Lin M, Liu T, Huang W, et al. Clinical benefit of rehabilitation training in spinal cord injury: a systematic review and meta-analysis. Spine. 2021;46:E398-410.
34. Senthilvelkumar T, Magimairaj H, Fletcher J, Tharion G, George J. Comparison of body weight-supported treadmill training versus body weight-supported overground training in people with incomplete tetraplegia: a pilot randomized trial. Clin Rehabil. 2015;29:42–9.
35. Li M, Mo J, Wu D, He H, Hu P. Treadmill training improves neural function recovery in rats with spinal cord injury via JAK2/STAT3 signaling pathway and attenuating apoptosis. NeuroReport. 2024;35:811–21.
36. Su H, Luo H, Wang Y, Zhao Q, Zhang Q, Zhu Y, et al. Myelin repair of spinal cord injury in adult mice induced by treadmill training upregulated peroxisome proliferator-activated receptor gamma coactivator 1 alpha. Glia. 2024;72:607–24.
37. Ageeva T, Sabirov D, Sufianov A, Davletshin E, Plotnikova E, Shigapova R, et al. the impact of treadmill training on tissue integrity, axon growth, and astrocyte modulation. IJMS. 2024;25:3772.
38. Lee D-H, Cao D, Moon Y, Chen C, Liu N-K, Xu X-M, et al. Enhancement of motor functional recovery in thoracic spinal cord injury: voluntary wheel running versus forced treadmill exercise. Neural Regen Res. 2025;20:836–44.
39. Davaa G, Hong JY, Kim TU, Lee SJ, Kim SY, Hong K, et al. Exercise ameliorates spinal cord injury by changing DNA methylation. Cells. 2021;10:143.
40. Xu X, Du H-Y, Talifu Z, Zhang C-J, Li Z-H, Liu W-B, et al. Glycine and N-acetylcysteine (GlyNAC) combined with body weight support treadmill training improved spinal cord and skeletal muscle structure and function in rats with spinal cord injury. Nutrients. 2023;15:4578.
41. Singh A, Balasubramanian S, Murray M, Lemay M, Houle J. Role of spared pathways in locomotor recovery after body-weight-supported treadmill training in contused rats. J Neurotrauma. 2011;28:2405–16.
42. Barrett JP, Aubrecht TG, Smith A, Vaida M, Henry RJ, Doran SJ, et al. Molecular pathway changes associated with different post-conditioning exercise interventions after experimental TBI. J Neurotrauma. 2024. https://doi.org/10.1089/neu.2024.0120.
43. Amorós-Aguilar L, Portell-Cortés I, Costa-Miserachs D, Torras-Garcia M, Riubugent-Camps È, Almolda B, et al. The benefits of voluntary physical exercise after traumatic brain injury on rat's object recognition memory: A comparison of different temporal schedules. Exp Neurol. 2020;326: 113178.
44. Goldshmit Y, Lythgo N, Galea MP, Turnley AM. Treadmill training after spinal cord hemisection in mice promotes axonal sprouting and synapse formation and improves motor recovery. J Neurotrauma. 2008;25:449–65.
45. Kiss Bimbova K, Bacova M, Kisucka A, Gálik J, Ileninova M, Kuruc T, et al. Impact of endurance training on regeneration of axons, glial cells, and inhibitory neurons after spinal cord injury: a link between functional outcome and regeneration potential within the lesion site and in adjacent spinal cord tissue. IJMS. 2023;24:8616.
46. Cieri MB, Ramos AJ. Astrocytes, reactive astrogliosis, and glial scar formation in traumatic brain injury. Neural Regen Res. 2025;20:973–89.
47. Anderson MA, Burda JE, Ren Y, Ao Y, O'Shea TM, Kawaguchi R, et al. Astrocyte scar formation aids central nervous system axon regeneration. Nature. 2016;532:195–200.
48. Perez-Gianmarco L, Kukley M. Understanding the role of the glial scar through the depletion of glial cells after spinal cord injury. Cells. 2023;12:1842.
49. Song BG, Kwon SY, Kyung JW, Roh EJ, Choi H, Lim CS, et al. Synaptic cell adhesion molecule 3 (syncam3) deletion promotes recovery from spinal cord injury by limiting glial scar formation. IJMS. 2022;23:6218.
50. Hong JY, Lee J, Kim H, Yeo C, Jeon W-J, Lee YJ, et al. Shinbaro2 enhances axonal extension beyond the glial scar for functional recovery in rats with contusive spinal cord injury. Biomed Pharmacother. 2023;168: 115710.
51. Trivedi A, Noble-Haeusslein LJ, Levine JM, Santucci AD, Reeves TM, Phillips LL. Matrix metalloproteinase signals following neurotrauma are right on cue. Cell Mol Life Sci. 2019;76:3141–56.
52. Bradbury EJ, Burnside ER. Moving beyond the glial scar for spinal cord repair. Nat Commun. 2019;10:3879.
53. Fan B, Wei Z, Feng S. Progression in translational research on spinal cord injury based on microenvironment imbalance. Bone Res. 2022;10:35.
54. Xu Y, He X, Wang Y, Jian J, Peng X, Zhou L, et al. 5-Fluorouracil reduces the fibrotic scar via inhibiting matrix metalloproteinase 9 and stabilizing microtubules after spinal cord injury. CNS Neurosci Ther. 2022;28:2011–23.
55. Ogier C, Bernard A, Chollet A, Le Diguardher T, Hanessian S, Charton G, et al. Matrix metalloproteinase-2 (MMP-2) regulates astrocyte motility in connection with the actin cytoskeleton and integrins. Glia. 2006;54:272–84.
56. Hsu JYC, Bourguignon LYW, Adams CM, Peyrollier K, Zhang H, Fandel T, et al. Matrix metalloproteinase-9 facilitates glial scar formation in the injured spinal cord. J Neurosci. 2008;28:13467–77.
57. Hsu JYC, McKeon R, Goussev S, Werb Z, Lee J-U, Trivedi A, et al. Matrix metalloproteinase-2 facilitates wound healing events that promote functional recovery after spinal cord injury. J Neurosci. 2006;26:9841–50.
58. Nathan F, Li S. Environmental cues determine the fate of astrocytes after spinal cord injury. Neural Regen Res. 2017;12:1964.
59. Yang T, Dai Y, Chen G, Cui S. Dissecting the dual role of the glial scar and scar-forming astrocytes in spinal cord injury. Front Cell Neurosci. 2020;14:78.
60. Tamaru T, Kobayakawa K, Saiwai H, Konno D, Kijima K, Yoshizaki S, et al. Glial scar survives until the chronic phase by recruiting scar-forming astrocytes after spinal cord injury. Exp Neurol. 2023;359: 114264.

Publisher's Note